Spectrochimica Acta Part A: Molecular and Biomolecular Spectroscopy 127 (2014) 225–230

Contents lists available at ScienceDirect

Spectrochimica Acta Part A: Molecular and Biomolecular Spectroscopy

journal homepage: www.elsevier.com/locate/saa

Characterization and biological activities of two copper(II) complexes with dipropylenetriamine and diamine as ligands

Mousa AL-Noaimi [a,*], Mohammad I. Choudhary [b,c], Firas F. Awwadi [d], Wamidh H. Talib [e], Taibi Ben Hadda [f], Sammer Yousuf [c], Ashraf Sawafta [g], Ismail Warad [h,*]

[a] Department of Chemistry, Hashemite University, P.O. Box 150459, Zarqa 13115, Jordan
[b] Department of Chemistry, Science College, King Saud University, P.O. Box 2455, Riyadh 11451, Saudi Arabia
[c] H.E.J. Research Institute of Chemistry, International Center for Chemical and Biological Sciences, University of Karachi, Karachi 75270, Pakistan
[d] Chemistry Department, Faculty of Science, The University of Jordan, Amman 11942, Jordan
[e] Department of Clinical Pharmacy and Therapeutics, Applied Science University, Amman 11931, Jordan
[f] Laboratoire LCM, Faculty of Sciences, University Mohammed 1ER, Oujda 60000, Morocco
[g] Biology and Biotechnology Department, AN-Najah National University, P.O. Box 7, Nablus, Palestine
[h] Department of Chemistry, AN-Najah National University, P.O. Box 7, Nablus, Palestine

HIGHLIGHTS

- Mixed-ligands $[Cu(dipn)(2N)]Br_2$ complexes are synthesized.
- The complexes have significant antimicrobial and antiproliferative activity.
- The electronic spectra of the complexes are explained by DFT and TDDFT.

GRAPHICAL ABSTRACT

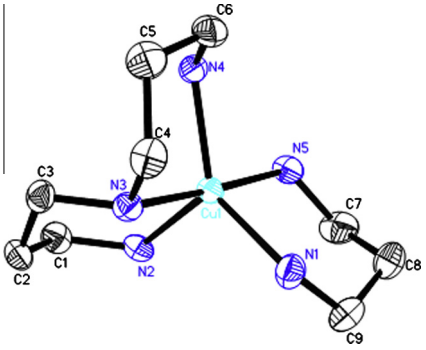

ARTICLE INFO

Article history:
Received 5 January 2014
Received in revised form 8 February 2014
Accepted 13 February 2014
Available online 22 February 2014

Keywords:
Cu(II) complexes
Polyamine ligands
Single-crystal XRD
Biological activity

ABSTRACT

Two new mixed-ligand copper(II) complexes, $[Cu(dipn)(N—N)]Br_2$ **(1–2)** [dipn = dipropylenetriamine, N—N = ethylenediamine (en) (**1**) and propylenediamine (pn) (**2**)], have been synthesized. These complexes were characterized by spectroscopic and thermal techniques. Crystal structure for **2** shows a distorted trigonal–bipyramidal geometry around Cu(II) ion with one solvate water molecule. Antimicrobial and antiproliferative assays were conducted to evaluate the biological activities of these complexes. The complexes exhibit a promising antimicrobial effect against an array of microbes at 200 μg/mL concentration. The antiproliferative assay shows a high potential of these complexes to target Human keratinocyte cell line with IC_{50} values of 155 and 152 μM. The absorption spectrum of **2** in water was modeled by time-dependent density functional theory (TD-DFT).

Introduction

The coordination chemistry of Cu(II), involving tridentate and bidentate amines ligands, attracted considerable interest due to their chelating properties [1]. The molecular structure of

* Corresponding authors. Tel.: +962 (5) 3903333; fax: +962 (5) 3826613 (M. AL-Noaimi).
E-mail address: manoaimi@hu.edu.jo (M. AL-Noaimi).

http://dx.doi.org/10.1016/j.saa.2014.02.016
1386-1425/

five-coordinated copper(II) complexes revealed an extensive variability, ranging from regular trigonal bipyramidal to regular square based pyramidal with most complexes displaying a structure that is intermediate between the two extremes. In such materials, interesting properties and potentials in spectroscopy, electrochemistry, biological activity and magnetism, etc. can be introduced from either the inorganic species or the organic linker molecules [2–6]. Although metal complexes with tridentate amine ligands, such as diethylenetriamine (dien) have been thoroughly investigated [7–11]. Complexes containing the analogous dipropylenetriamine (dipn) ligand have not received much attention, interestingly no report on the synthesis of copper(II) complexes containing the dipropylenetriamine, along with any daimine is found in literature.

Copper(II) complexes have found possible medical uses in the treatment of many diseases including cancer [12,13]. It has been known that the anti-cancer activity of some copper(II) complexes may be based on their ability to inhibit DNA synthesis [12]. These complexes are expected to be permeable through the cell membrane [14,15]. The determination of the structure of these complexes in solution is indispensable for the understanding of some biological processes including, the participation of metals in the processes of replication and transcription of nucleic acid [16,17]. The coordination properties of the polyamines presented in biological systems are important for the role that they play in various cell processes [18]. The antitumor activity in the presence of plasma amineoxidase, requires a terminal NH_2—$(CH_2)_3$—NH group and at least three carbon atoms between the primary and secondary amino groups [19], while the antimicrobial action is based on the ability to serve as an effective chelating agent [20].

Herein, we report the synthesis and the spectroscopic investigation of two new complexes, [Cu(dipn)(N—N)]Br_2 (**1**–**2**) [dipn = dipropylenetriamine, N—N = ethylenediamine (en) (**1**) and propylenediamine (pn) (**2**)] and a single crystal X-ray structure of **2**. Biological studies on these complexes are also reported. The absorption spectrum of **2** in water was modeled by time-dependent density functional theory (TD-DFT).

Experimental

Materials and physical measurements

All the reagents were of analytical grade and purchased from Sigma–Aldrich and used as received. Elemental analyses were recorded with an Elementar Varrio EL analyzer. The FT-IR spectra (4000–200 cm^{-1}) were obtained from KBr discs with a Perkin–Elmer 621 spectrophotometer. Thermal analyses were carried out with TA instrument SDT-Q600 in air. Electronic spectra were recorded in water at room temperature on Pharmacia LKB-Biochrom 4060 spectrophotometer. FAB-MS data were obtained a Finnigan 711A (8 kV), modified by AMD and reported as mass/charge (m/z), respectively.

*Synthesis of [Cu(dipn)(N—N)]Br_2 (**1–2**), general procedure*

An ethanolic solution (10 mL) of dipropylenetriamine (1.5 mmol) and diamine (1.5 mmol) were mixed together and added drop-wise to $CuBr_2$ (1.5 mmol), dissolved in 10 mL of (50%) ethanol. The resulting reaction mixture was stirred for 3 min. The reaction mixture was subjected to ultrasound waves for 5–20 min until the blue precipitates appeared. The solid was filtered and carefully washed with dichloromethane, then dried under vacuum. Crystals of **2** suitable for X-ray structural analysis have been obtained by slow evaporation of EtOH/water solution of the complex.

*[Cu(dipn)(en)]Br_2 (**1**)*

$CuBr_2$ (0.33 g, 1.51 mmol) was treated with dipn (0.25 g, 1.51 mmol) and en (0.09 g, 1.5 mmol) to produce [Cu(dipn)(en)]Br_2 as a blue powder. Yield (0.54 g, 90%), M.p. = 215 °C. MS m/z 415.2 [M+] for$C_8H_{25}N_5Br_2Cu$ Calculated: C, 23.17; H, 6.08; N, 16.89. Found C, 23.35; H, 6.10; N, 16.62%, IR (KBr, νcm^{-1}):3450 (ν_{O-H}), 3370 and 3290, (ν_{H-N}), 2920 (ν_{C-H}), 1560 (ν_{N-H}), 1180 (ν_{N-C}), 630 and 530(ν_{Cu-N}). UV–Vis in water: $\lambda_{max}(\varepsilon_{max}/M^{-1}\,cm^{-1})$: 255 ($1.45 \times 10^3$), 575 ($3.40 \times 10^2$).

*[Cu(dipn)(pn)]Br_2 (**2**)*

$CuBr_2$ (0.33 g, 1.51 mmol) was treated with dipn (0.25 g, 1.51 mmol) and pn (0.11 g, 1.5 mmol) to produce [Cu(dipn)(pn)]Br_2 as blue crystals. Yield (0.56 g, 87%). M.p. = 250 °C. MS m/z 428.2 [M^+] for for$C_9H_{27}N_5Br_2Cu$. H_2O Calculated: C, 24.20; H, 6.54; N, 15.60. Found C, 24.35; H, 6.50; N, 15.42%. IR (KBr, νcm^{-1}):3420 (ν_{O-H}), 3380 and 3260 (ν_{H-N}), 2940 (ν_{C-H}), 1550 (ν_{N-H}), 1190 (ν_{N-C}), 620 and 510 (ν_{Cu-N}). UV–Vis in water: $\lambda_{max}(\varepsilon_{max}/M^{-1}\,cm^{-1})$: 270 ($1.35 \times 10^3$), 582 ($2.50 \times 10^2$).

Single-crystal X-ray data collection

Crystals of complex **2** were grown by a slow evaporation of water/EtOH solvent mixture. A blue crystal ($0.40 \times 0.20 \times 0.02$ mm) was used for data collection on Bruker SMART APEX II CCD diffractometer using Mo Kα radiation with a fine focus tube with 50 kV and 30 mA. The structure (Fig. 1) was solved by the direct methods and refined by a full-matrix least-square calculation on F2 by using SHELXTL program package [21]. All non-hydrogen atoms are refined anisotropically. Carbon attached hydrogen atoms are placed in the calculated position and refined using riding model. Hydrogen atoms attached to oxygen and nitrogen are located using Fourier difference map and isotropically refined. The isotropic thermal displacement parameters of these hydrogen are set to 1.2 of that of the parent atoms.

Antimicrobial assay

The antimicrobial activity of the two complexes were tested against the following microbial strains: *Escherichia coli* (ATCC 25922), *Staphylococcus aureus* (ATCC 25213), *Bacillus subtilis* (ATCC 6633), a *Micrococcus luteus* (ATCC 10420), and *Candida albicans*

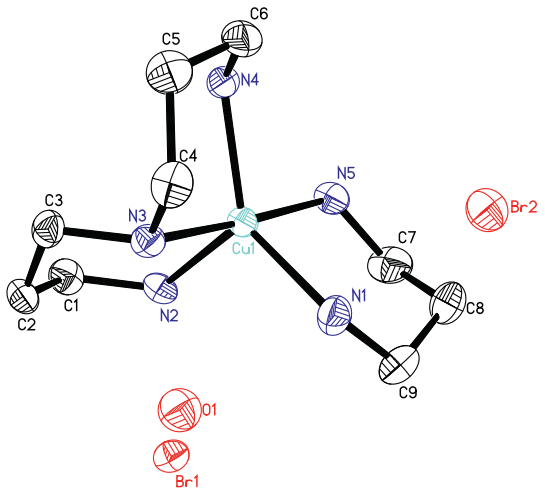

Fig. 1. The ORTEP generated diagram of **2** with displacement ellipsoids drawn at 30% probability level. Hydrogen atoms are omitted for clarity.

(ATCC 10231), Bacterial strains were stocked onto nutrient agar slant and *C. albicans* was stocked onto malt agar slant. All slants were stored at 4 °C. Disc diffusion method was used to study the antimicrobial activity of the synthesized complexes [22,23]. Stock complexes were initially dissolved in water and sterilized by filtration using 0.45 μm membrane filters. Sterile 6 mm diameter filter paper disc was soaked with 0.2 mg/disc of each sterile complex and was placed in triplicates onto Muller–Hinton agar (Oxoid, England) plates for bacterial strains and malt extract agar for *C. albicans*. These plates were previously inoculated separately with 100 μL (1.0×10^8 CFU m L^{-1}) of fresh culture of bacteria or yeast cells suspension. The plates were incubated for 24 h at 37 °C (for bacteria) or for 48–72 h at 28 °C (for *C. albicans*). After incubation, the inhibition zone around each disc was measured and recorded. Reported inhibition zones are the average calculated from three replicates. Discs soaked with sterile water were used as a negative control. While standard antibacterial tetracycline (30 μg/disc) and antifungal nystatin (100 μg/disc) (Oxoid, Basingstoke, UK) were used as positive controls in the assay. In order to exclude any antimicrobial activity that may result from copper bromide and the ligands, sterile discs were soaked with each compound and tested against the same microbial strains. The concentrations of each compound ($CuBr_2$ and ligands) was adjusted to be equal to the concentration of corresponding the complex.

Antiproliferative assay

Human keratinocyte cell line (HaCaT) was used to test the potential antiproliferative activity of our complexes. Cells were cultured in Minimum Essential Medium Eagle (Gibco, UK) supplemented with 10% heat inactivated fetal bovine serum (Gibco, UK), 29 μg/mL L-glutamine, and 40 μg/ml Gentamicin. The *in vitro* antiproliferative activity of the newly synthesized complexes against Human keratinocyte cell line (HaCaT) was measured using the MTT assays [24,25]. This assay detects the reduction of MTT by mitochondrial dehydrogenase to blue formazan product, which reflects the normal function of mitochondria and cell viability [24]. The cells were plated in 96-well culture plates at a density of 5000 cells per well and incubated for 24 h at 37 °C in a 5% CO_2 incubator. After 24 h incubation, a partial monolayer was formed then the media was removed and 200 μL of the medium containing the complex (initially dissolved in water) were added and re-incubated for 48 h. After that, the cells were treated with 10% (v/v) MTT dye solution (5 mg/mL) for 4 h. After incubation, the media were replaced with DMSO solution (150 μL) to dissolve the dye and the absorbance was measured at 570 nm, using an Absorbance Plate Reader (Bio-Rad). Stock solutions of complexes were prepared in distilled water, sterilized using 0.2 μm membrane filters, and diluted using culture media. The following concentrations were prepared for each complex 2.5, 10, 40, 80, 160, and 200 μM. Untreated cells were used as a negative control while cells treated with *cis*-platin were used as a positive control. The antiproliferative effect of the tested complexes was determined by comparing the optical density of the treated cells against the optical density of the control (untreated cells). IC_{50} values were calculated as the concentrations that show 50% inhibition of proliferation.

Theoretical calculations

Full geometry optimization of **2** was carried out using density functional theory (DFT) at the B3LYP level [25]. All calculations were carried out using the GAUSSIAN 09 program package with the aid of the GaussView visualization program [26]. For C, H and N the cc-pVDZ basis set were assigned, while for Cu, the LanL2DZ basis set with effective core potential were employed [27]. Vertical electronic excitations based on B3LYP optimized geometries were computed using the time-dependent density functional theory (TD-DFT) formalism in water using polarizable continuum model (PCM) [28–31]. Gauss Sum was used to calculate the fractional contributions of various groups to each molecular orbital [32].

Result and discussion

Mixed-ligand copper(II) complexes of the type [Cu(dipn)(N-N)]Br_2 (**1**–**2**), dipn is dipropylenetriamine (dipn) and (N-N) is ethylenediamine (en) (**1**) and propylamine (pn) (**2**), were synthesized by the reaction of amines ligands with Cu(II) ions in [1:1:1] molar ratio in a mixture of ethanol: water (Scheme 1). These complexes have been isolated as bromide salts in good yields. They have been characterized using elemental analysis and spectral methods. Theses complexes are blue in color and are soluble in water. The X-ray crystal structure of **2** reveals distorted trigonal–bipyramidal geometry for the CuN_5 chromophore.

IR spectral data

The IR spectra of complex **2** and the free propylamine (pn) and dipropylenetriamine (dipn) ligands have been recorded (Fig. S1A). The prominent bands observed in the IR spectra of Cu(II) complexes are presented in the experimental section. The absorption band around 1050 cm^{-1} is probably due to the stretching vibration of carbon–nitrogen bond [33]. The strong bands at around 1400 cm^{-1} are very likely associated with the scissoring vibration of —CH_2— groups [34]. The band at 730–790 cm^{-1} may be due to the rocking vibration of CH_2 groups [34]. In the spectra of the complexes **1** and **2** the three bands at 3310–3413, 3235–3266 and 1583–1616 cm^{-1} assigned to ν_s(N–H), ν_{as}(N–H) and δ(N–H), respectively are shifted to wavenumbers lower than those encountered in the free 1,2-diamines or triamines, confirming the coordination of the amine groups with copper [35]. As the lone pair of electrons of the donor nitrogen atoms become involved in the metal–ligand bond, the transfer of electron density to the metal and the subsequent polarization of the ligands involves electron depopulation of the N—H bond, which culminates in a shift to lower frequencies [33,34]. Appearance of a band at 510 cm^{-1} was due to $\nu_{(Cu-N)}$ vibrations [36]. A band appeared in the 292–295 cm^{-1} region was assigned to the $\nu_{(Cu-Br)}$ vibration [37]. Meanwhile the peaks at 3520 $\nu_{(O-H)}$(O—H) and 1426 $\nu_{(bend)}$are the characteristic bands of H_2O which indicates the existence of molecular lattice water.

Thermogravimetric analyses

The thermal stabilities of the complexes were investigated by TG/DTA. The TGA curves were obtained at a heating rate of 10 °C min^{-1} in air atmosphere over the temperature range of 0–1000 °C. The thermogravimetric analyses of these complexes revealed the occurrence of three consecutive processes, namely dehydration, ligand pyrolysis and inorganic residue formation.

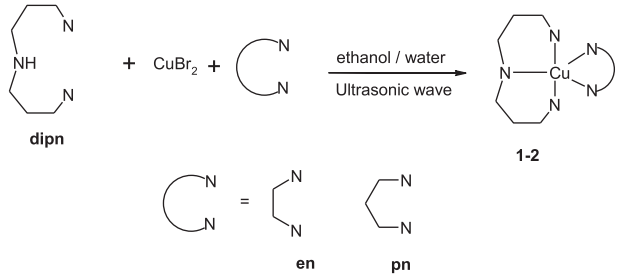

Scheme 1. Synthesis of mixed-ligand Cu(II) complexes.

The desired Cu(II) complexes showed similar thermogravimetric behavior, the TG/DTA spectra of **2** illustrated mainly the expected three steps of weight loss. First step was losing uncoordinated water molecule at endothermic sign of DTA at 107 °C. The second decomposition stage from 160 °C and end at 480 °C losing around 40% of weigh, triamine lose with two DTA exothermic signs at 250 and 480 °C with expected final product of this step is $CuBr_2$. The third step starts from 480 °C and end at 720 °C which lead to the removal of bromide ions of $CuBr_2$ to form copper oxide (Cu=O) final product with sharp weight loss. The final residue was analyzed by IR spectra and identified as Copper oxide (CuO, 22%).

*Crystal structure for complex **2***

Complex **2** crystallizes in the Orthorhombic $P2_12_12_1$ space group. The crystal data and structure refinement parameters are given in Table 1. Selected bond angles and bond distances are given in Table 2. The ORTEP diagram of the molecule with the atomic numbering is shown in Fig. 1. The Copper atom is coordinated in a distorted trigonal–bipyramidal geometry with one triamine (dipn) and one bidentate diamine (pn) ligands and one water molecule as solvate [38]. In the five coordinate structures, the dipn ligand displays axial–equatorial coordination. The N_1N_5-donor atoms of pn ligand occupy the basal plane (the ligand bite angle is 110.56(13)°]. The Cu—N bonds length (range 2.034–2.132 Å) are comparable with the other structurally similar copper(II) complexes [39,40]. For assessing the degree of trigonality in five-coordinate transition metal complexes, the expression formulated by Addison et al. [41], $\tau = (\beta - \alpha)/60$, where τ is the index of trigonality within the structural continuum between ideal trigonal bipyramidal and square-pyramidal was used. The limiting cases are $\tau = 0$ for perfectly square-pyramidal geometry and $\tau = 1$ for perfectly trigonal bipyramidal geometry. In our compound **2**, the τ factor takes a value of 0.69 [where β = N2—Cu3—N4 175.44° and α = N3 Cu3 N5 134.10°] indicating a significant distortion.

Comparison of the optimized molecular structure of complex **2** with that of the experimentally, reveals that Cu—N bond distances in the optimized structure are always longer than the experimentally determined analog (avg. = 0.08 Å) (Table 2). However, the relative length follow the similar trend in the two structures with one exception; Cu3—N1 is longer than Cu3—N5 in the experimentally determined structure, in contrast, Cu3—N5 is longer than Cu3—N1 in the optimized structure. This can be explained based on intermolecular forces, the optimized structure rules out the effect of intermolecular interactions, it has been found intermolecular forces play a major role in determining the final structure in solid state [42]. Also, Cu3—N2 bond distance is the shortest in both the optimized and experimentally determined structure, this is expected, since N—N is a secondary nitrogen and hence a better electron donor. Generally, the bond angles in optimized structure agree with the experimentally determined ones (Table 2). The differences in N—Cu—N angles are hard to rationalize due to the presence of too many N—H...Br and N—H...O hydrogen bonding interactions.

Three types of hydrogen bonding interactions stabilized the final three dimensional structure; N—H...Br, N—H...O and O—H...Br. The data summarizing these interactions are listed in Table 3. N—H...Br hydrogen bonding interactions connect the cations and anions to form chain structures run parallel to b axis (Fig. S2A), subsequently, these chains are linked *via* O—H...Br and N—H...O to form the final 3D structure (Fig. S2B)

Table 1
Crystallographic data and structure refinement parameters for **2**.

Empirical formula	$C_9H_{29}Br_2CuN_5O$
Formula weight	446.73
Temperature	100 K
Wavelength (Å)	0.71073
Crystal system	Orthorhombic
Space group	$P2_12_12_1$
Unit cell dimensions (Å)	a = 9.0358(8), b = 13.4316(12), c = 14.0195(13)
Volume (Å^3)	1701.5(3)
Z	4
Density (calculated)	1.744 Mg/m^3
Absorption coefficient mm^{-1}	5.979
F(000)	900
Crystal size (mm^3)	0.35 × 0.21 × 0.09
θ range for data collection (°)	2.1 to 26.43
Index ranges	$-11 \leqslant h \leqslant 11$, $0 \leqslant k \leqslant 16$, $0 \leqslant l \leqslant 17$
Reflections collected	13481
Independent reflections	3495 [R_{int} = 0.0424]
Data/restraints/parameters	3493/1/196
Completeness to theta = 25.00°	100%
Absorption correction	Multi-scan
Goodness-of-fit on F^2	0.992
Final R indices [I > 2sigma(I)]	R_1[a] = 0.0275, wR_2[b] = 0.0468
R indices (all data)	R_1[a] = 0.0329, wR_2[b] = 0.0481
Largest diff. peak and hole (e Å^{-3})	0.415 and −0.334
CCDC	979301

[a] $R_1 = \Sigma||Fo| - |Fc||/|\Sigma|Fo|$.
[b] $wR_2 = \{\Sigma w(Fo2 - Fc^2)^2/\Sigma w(Fo^2)^2\}^{1/2}$.

Table 2
Bond lengths [Å] and angles [°] for complex **2**.

	Experimental	Calculated
Bond lengths [Å]		
Cu3 N2	2.034(3)	2.0943
Cu3 N4	2.035(3)	2.0799
Cu3 N3	2.083(3)	2.1615
Cu3 N5	2.102(3)	2.2157
Cu3 N1	2.132(3)	2.1735
Bond angles [°]		
N2 Cu3 N4	175.44(12)	178.62
N2 Cu3 N3	88.88(12)	88.96
N4 Cu3 N3	88.11(12)	89.99
N2 Cu3 N5	87.80(13)	92.32
N4 Cu3 N5	91.81(13)	87.42
N3 Cu3 N5	134.04(13)	119.63
N2 Cu3 N1	91.50(11)	89.58
N4 Cu3 N1	92.92(12)	91.76
N3 Cu3 N1	115.28(13)	126.99
N5 Cu3 N1	110.56(13)	113.37

Visible and ultraviolet spectral data

The electronic absorption spectra are measured at room temperature in water, and the experimental absorption bands are assigned using the time-dependent DFT method. UV–Visible electronic absorption spectrum of complex (**1**–**2**) were measured in H_2O. The experimental absorption spectra of the complex **2** is shown in Fig. 2. Complex **2** has two bands, weak transitions around

Table 3
Hydrogen bonds parameters for **2** [Å and °].

D—H...A	d(D—H)	d(H...A)	d(D...A)	<(DHA)
O(1)—H(2O)...Br(2)#1	0.77(4)	2.66(4)	3.313(3)	144(4)
N(2)—H(2 N)...O(1)	0.82(3)	2.27(3)	3.067(4)	164(3)
N(5)—H(52 N)...O(1)	0.79(3)	2.26(3)	3.012(4)	159(3)
N(4)—H(41 N)...Br(1)#2	0.89(4)	2.64(4)	3.494(3)	163(3)
N(4)—H(42 N)...Br(2)#3	0.88(4)	2.61(4)	3.452(3)	160(3)
N(5)—H(51 N)...Br(2)#4	0.87(4)	2.63(4)	3.479(3)	169(3)
N(1)—H(11 N)...Br(1)#5	0.87(4)	2.58(4)	3.438(3)	166(3)
N(1)—H(12 N)...Br(2)#3	0.89(4)	2.61(4)	3.458(3)	160(3)
O(1)—H(1O)...Br(1)#5	0.789(18)	2.64(2)	3.413(3)	165(4)

Symmetry transformations used to generate equivalent atoms:
#1 $x-1, y, z-1$ #2 $x+1/2, -y+3/2, -z+1$ #3 $-x+3/2, -y+2, z-1/2$.
#4 $x-1/2, -y+3/2, -z+1$ #5 $-x+1/2, -y+2, z-1/2$.

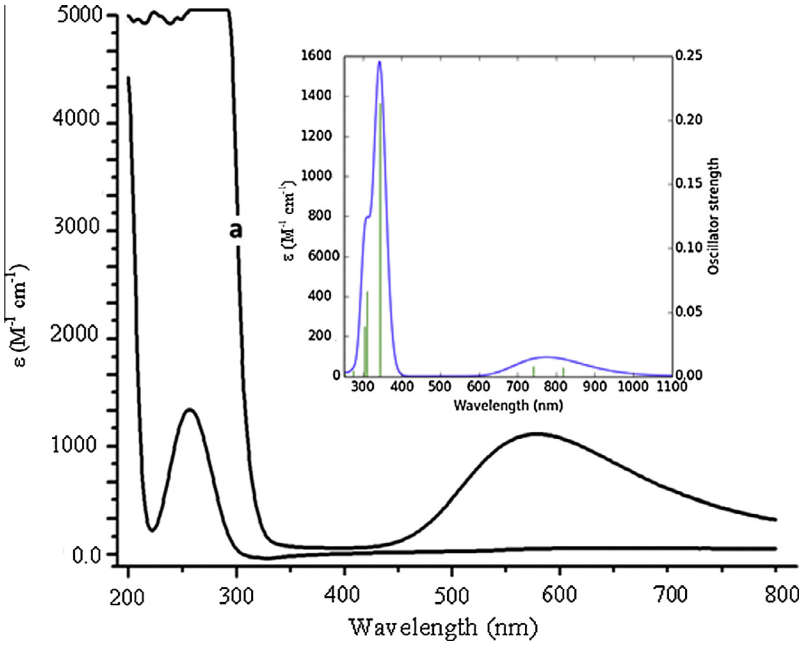

Fig. 2. UV–Vis spectrum of **2** in water, Inset shows simulated absorption spectrum, (green line) based on TD-DFT calculations, compared to excitation energies and oscillator strengths. (For interpretation of the references to color in this figure legend, the reader is referred to the web version of this article.)

λ_{max} = 575 and a strong transition around 225 nm. The assignment of the transitions in the UV–Visible region is supported by the TD-DFT calculations on complex **2**.

Energy level correlations along with the Relative percentages of atomic contributions to the lowest unoccupied and highest occupied molecular orbitals of the Cu, triamine and Pn ligands have been placed in Table S1. Moreover, the isodensity plots for the HOMOs and LUMOs orbitals are shown in Fig. S3. For complex **2**, the β-spin occupied orbitals mainly take part in electronic transitions. The β-spin from LUMO to LUMO + 3 have more than 60% Cu(dp), while LUMO + 4 to LUMO + 2 have more than 50% of triamine 25% of diamine ligands (Table S2). The β-spin HOMO to HOMO − 2 have Cu and/or triamine character, with only 10–13% contribution of Cu(dp) are in HOMO − 3 to HOMO − 6.

Computation of 20 excited states of complex **2** allowed the interpretation of the experimental spectra for the complexes in the 200–1000 nm range (Fig. 2). The calculated energy of excitation states and transition oscillator strength (*f*) are shown in Table S2. The absorption spectrum of **2** was simulated using Gauss Sum software [32] based on the obtained TD-DFT results. Both the experimental UV–Visible and its simulated absorption spectra in water shown in Fig. 2 are in acceptable agreement.

On the basis of its intensity and position, the high intensity and energy band at 225 nm result from the overlap of two transitions 309 (calculated) resulted from H-1/-6 to L(β) (Table S2) and ~343 nm (calculated) resulted from H/-2(β) to L(β)) thus this band is assigned as to N(p) → Cu(II) LMCT transition. The lowest energy band at 575 nm resulted from the overlap of two transitions, 741 nm (calculated) resulted from H-1/-6 to L(β) and 817 nm resulted from H(β) → L(β), thus this band is a assigned to a mixture of LMCT and d–d transition of Cu(II) ions which is typical for a distorted trigonal–bipyramidal coordination geometry around copper(II) [43].

Antimicrobial assay

The fundamental role of copper and the recognition of its complexes as important bioactive compounds *in vitro* and *in vivo* aroused an ever-increasing interest in these agents as potential drugs for therapeutic intervention in various diseases [44]. In order to evaluate the antimicrobial activity, the synthesized complexes were tested against several microbial strains (*E. coli, S. aureus, M. luteus, B. subtilis* and *C. albicans*). The highest activity of complex **2** was against *C. albicans* with inhibition zone of 18.5 mm. The same complex exhibited moderate activity against *E. coli* and *M. luteus* with inhibition zones of 14.4 and 16.0 mm, respectively. Weak activity of complex **2** was observed against *S. aureus* and *B. subtilis* with inhibition zones less than 12.7 mm (Table S3). More potent antimicrobial activity was detected for complex **2** which exhibited high activity against *S. aureus* and *M. luteus* (inhibition zone above 20 mm), moderate activity against *C. albicans* (inhibition zone of 16.4 mm), and weak activity against both *E. coli* and *B. subtilis* (inhibition zones less than 12.8 mm) (Table S3). Both complexes were able to target Gram positive and Gram negative bacteria in addition to the yeast *C. albicans* indicating a broad spectrum antimicrobial activity for these complexes. Such broad spectrum activity could be mediated by targeting essential steps in microbial growth or by causing metabolic toxicity [45]. It is good that mentioned that both $CuBr_2$ and the polyamine ligands did not show any antimicrobial activity under the same concentration with complexes (**1**–**2**). Our results are consistent with the previous findings that reported a broad antimicrobial activity of copper complexes against an array of pathogens [40]. The percentage mortality from opportunistic fungal infections is higher than 50% and may reach 95% in bone marrow transplant patients [46]. The commonly used antifungal drugs have high toxicity and limited spectrum [47]. Thus, there is a need for the synthesis of new antifungal agents. In this context, our complexes exhibited promising antifungal activity against *C. albicans* and our results agree with the previously published results that showed a potential of copper complexes to target different fungal strains [48].

Antiproliferative assay

The antiproliferative potential of complexes under study was evaluated using Human keratinocyte cell line. Both complexes exhibited promising antiproliferative activity against the tested cell line with IC_{50} values of 155 and 152 μM for complexes **1** and

2, respectively. These values are promising if compared with the IC_{50} value of the well-known anticancer agent *cis*-platin which has IC_{50} value of 144 μM against the same cell line. However, further testing is needed to study the potential antiproliferative activity of our complexes on different cancer cell lines, to determine their toxicity on normal cells, and to provide details about the mechanism of action of these compounds.

Conclusions

Two mixed-ligand dipropylenetriamine/diamines Cu(II) complexes were synthesized in high yields through a one pot ultrasonic reaction. Single crystal X-ray diffraction for complex **2** showed that copper atom is coordinated to amines ligands as bromide salt in a distorted trigonal–bipyramidal geometry with τ factor takes a value of 0.69. The structures of the desired complexes were determined by several available physical measurements, EA, FAB-MS, IR, UV–Vis, TG/DTA, CV and. The antimicrobial and antiproliferative studies revealed that our newly synthesized complexes have the potential to be utilized in health care facilities. The absorption spectrum of representative complex in water was modeled by time-dependent density functional theory (TD-DFT).

Acknowledgements

M. Al-Noaimi and I. Warad would like to thank the Hashemite University, Jordan and AN-Najah National University for their research support.

Appendix A. Supplementary material

Supplementary data associated with this article can be found, in the online version, at http://dx.doi.org/10.1016/j.saa.2014.02.016.

References

[1] F.A. Cotton, B. Hong, Prog. Inorg. Chem. 40 (1992) 179–289.
[2] R.D. Hancock, L.J. Bartolotti, Inorg. Chem. 44 (2005) 7175–7183.
[3] G. Murphy, P. Nagle, B. Murphy, B. Hathaway, J. Chem. Soc. Dalton Trans. (1997) 2645–2652.
[4] E.C. O'Brien, E. Farkas, M.J. Gil, D. Fitzgerald, A. Castineras, K.B. Nolan, J. Inorg. Biochem. 79 (2000) 47–51.
[5] B.-Q. Ma, S. Gao, T. Yi, C.-H. Yan, G.-X. Xu, Inorg. Chem. Commun. 3 (2000) 93–95.
[6] J.-C. Hierso, R. Amardeil, E. Bentabet, R. Boussier, B. Gautheron, P. Meunier, P. Kalck, Coord. Chem. Rev. 236 (2003) 143–206.
[7] R.N. Patel, H.C. Pandey, K.B. Pandeya, Ind. J. Chem. 36 (A) (1997) 809–811.
[8] R.N. Patel, K.B. Pandeya, Trans. Met. Chem. 24 (1999) 35–37.
[9] R.N. Patel, A.P. Patel, K.B. Pandeya, Ind. J. Chem. 38 (A) (1999) 900–905.
[10] R.N. Patel, N. Singh, R.P. Shrivastava, S. Kumar, K.B. Pandeya, J. Mol. Liq. 49 (2000) 95–99.
[11] B. Kurzak, K. Bogusz, D. Kroczewska, J. Jezierska, Polyhedron 20 (2001) 2627–2636.
[12] R.J. Sorenson, Chem. Br. 16 (1984) 1110–1113.
[13] R.K. Gouch, T.W. Kensler, L.W. Oberley, J.R.J. Sorenson, in: K.D. Karlin, J. Zobista (Eds.), Biochemical and Inorganic Copper Chemistry, vol. 1, Adenine, New York, 1986, pp. 139–156.
[14] M.J. Chare, P.C. Hydes, in: H. Sigel (Ed.), Metal Ion in Biological Systems, vol. 2, Marcel Dekker, New York, 1980, pp. 1–62.
[15] K. Takamiya, Nature (London) 185 (1960) 190.
[16] P. Kopf-Maier, H. Kopf, Chem. Rev. 87 (1987) 1137–1152.
[17] S.E. Scherman, S.J. Lippard, Chem. Rev. 87 (1987) 1153–1181.
[18] U. Bachrach, Function of Naturally Occurring Polyamines, Academic Press, NY and London, 1973.
[19] M. Israel, E.J. Modest, J. Med. Chem. 14 (1971) 1042–1046.
[20] E.D. Weinberg, Antimicrob. Agents Chemother. (1963) 573–576.
[21] REF((d) SHELXTL, v. 6.10; Structure Determination Software Suite; Sheldrick, G.M., Bruker (Ed.), AXS Inc.: Madison, WI, 2001.
[22] J.K. Hurst, Coord. Chem. Rev. 249 (2005) 313–328.
[23] D. Chatterjee, A. Mitra, R.E. Shepherd, Inorg. Chim. Acta 357 (2004) 980–990.
[24] C.S. Lau, C.Y. Ho, C.F. Kim, K.N. Leung, K.P. Fung, T.F. Tse, H.L. Chan, M.S. Chow, Life Sci. 75 (2004) 797–808.
[25] C. Lee, W. Yang, R.G. Parr, Phys. Rev. B. 37 (1988) 785–789.
[26] Gaussian 09, Revision A.1, M.J. Frisch, G.W. Trucks, H.B. Schlegel, G.E. Scuseria, M.A. Robb, J.R. Cheeseman, G. Scalmani, V. Barone, B. Mennucci, G.A. Petersson, H. Nakatsuji, M. Caricato, X. Li, H.P. Hratchian, A.F. Izmaylov, J. Bloino, G. Zheng, J.L. Sonnenberg, M. Hada, M. Ehara, K. Toyota, R. Fukuda, J. Hasegawa, M. Ishida, T. Nakajima, Y. Honda, O. Kitao, H. Nakai, T. Vreven, J.A. Montgomery, Jr., J.E. Peralta, F. Ogliaro, M. Bearpark, J.J. Heyd, E. Brothers, K.N. Kudin, V.N. Staroverov, R. Kobayashi, J. Normand, K. Raghavachari, A. Rendell, J.C. Burant, S.S. Iyengar, J. Tomasi, M. Cossi, N. Rega, J.M. Millam, M. Klene, J.E. Knox, J.B. Cross, V. Bakken, C. Adamo, J. Jaramillo, R. Gomperts, R.E. Stratmann, O. Yazyev, A.J. Austin, R. Cammi, C. Pomelli, J.W. Ochterski, R.L. Martin, K. Morokuma, V.G. Zakrzewski, G.A. Voth, P. Salvador, J.J. Dannenberg, S. Dapprich, A.D. Daniels, O. Farkas, J.B. Foresman, J.V. Ortiz, J. Cioslowski, D.J. Fox, Gaussian Inc, Wallingford CT, 2009. GaussView5.0.9, Gaussian: Pittsburgh, PA.
[27] P.J. Hay, W.R. Wadt, J. Chem. Phys. 82 (1985) 270–283.
[28] R. Bauernschmitt, R. Ahlrichs, Chem. Phys. Lett. 256 (1996) 454–464.
[29] M.K. Casida, C. Jamorski, K.C. Casida, D.R. Salahub, J. Chem. Phys. 108 (1998) 4439–4449.
[30] R.E. Stratmann, G.E. Scuseria, M.J. Frisch, J. Chem. Phys. 109 (1998) 8218–8224.
[31] M. Cossi, N. Rega, G. Scalmani, V. Barone, Comput. Chem. 24 (2003) 669–681.
[32] N.M. O'Boyle, A.L. Tenderholt, K.M. Langner, J. Comput. Chem. 29 (2008) 839–845.
[33] P. Vijayan, P. Vijayaraj, P. Setty, C. Hariharpura, A. Godavarthi, S. Badami, D. Arumugam, S. Bhojraj, Biol. Pharm. Bull. 24 (2004) 528–530.
[34] C. Tsiamis, M. Themeli, Inorg. Chim. Acta 206 (1993) 105–115.
[35] S. Destri, M. Pasini, W. Porzio, F. Rizzo, G. Dellepiane, M. Ottonelli, G. Musso, F. Meinardi, L. Veltri, J. Lumin. 127 (2007) 601–605.
[36] K. Nakamoto, Infrared and Raman spectra of Inorganic and Coordination Compounds, 4th ed., J. Wiley & Sons, NY, 1986.
[37] A. Cassol, P. Di Bernardo, R. Portanova, M. Tolazzi, G. Tomat, P. Zanonato, J. Chem. Soc. Dalton Trans. (1992) 469–474.
[38] A.W. Addison, T. Nageswara-Rao, J. Reedijk, J. van Rijn, G.C. Verschoor, J. Chem. Soc. Dalton Trans. (1984) 1349–1356.
[39] G. Tabbi, W.L. Driessen, J. Reedjik, R.P. Bonomo, N. Weldman, A.L. Spek, Inorg. Chem. 36 (1997) 1168–1175.
[40] R.N. Patel, N. Singh, K.K. Shukla, J. Niclós-Gutiérrez, A. Castineiras, V.G. Vaidyanathan, B. Unni Nair, Spectrochim. Acta Part A 62 (2005) 261–268.
[41] G. Huang, C. Su, S. Wang, F. Liao, K. Lin, J. Coord. Chem. 43 (2000) 211–226.
[42] F.F. Awwadi, S.F. Haddad, B. Twamley, R.D. Willett, CrystEngComm 14 (2012) 6761–6769.
[43] C.W. Liu, R.J. Staples, J.P. Fackler, Coord. Chem. Rev. 174 (1998) 147–177.
[44] I. Iakovidis, I. Delimaris, S.M. Piperakis, Mol. Biol. Int. 20 (2011). Article ID594529.
[45] D. Srinivasan, S. Nathan, T. Suresh, L.P. Perumalsamy, J. Ethnopharmacol. 74 (2001) 217–220.
[46] L.O. Regasini, F. Cotinguiba, A.A. Morandim, M.J. Kato, L. Scorzoni, M.J. Mendes-Gianni, V.S. Bolzani, M. Furian, J. Biotechnol. 8 (2009) 2866–2870.
[47] E.J. Helmerhorst, I.M. Reijnders, W.V.T. Hof, I.S. Smith, E.C.J. Veerman, A.V.N. Amerongen, Antimicrob. Agents Chemother. 43 (1999) 702–704.
[48] R.N. Patel, Nripendra Singh, K.K. Shukla, U.K. Chauhan, J. Niclos-Gutierrez, A. Castineiras, Inorg. Chim. Acta 357 (2004) 2469–2476.